The Influence of Precursor Temperature on The Properties of Erbium-Doped Zirconium Telluride Thin Film Material Via Electrochemical Deposition

Ikhioya I. Lucky[1*] Ezeorba M. Chigozirim [1], Okoroh Doris O[3], Anene C. Rita[2] and Obasi C. Ogonnaya[1*].

[1]*Department of Physics and Astronomy, University of Nigeria, Nsukka 410001, Nigeria*
[2]*Department of Physics and Industrial Physics, Nnamdi Azikiwe University, Awka, Nigeria*
[3]*Federal College of Education (Technical), Omoku, River State.*

Abstract
The study of the influence precursor temperature on the structural, morphological and optical properties of erbium doped zirconium telluride using ECD method where the aqueous solution of the cationic precursor was 0.1 mol solution of $ZrOCl_2.8H_2O$ and the anionic precursor was 0.01 mol solution of Tellurdioxide (TeO_2) was prepared by dissolving with 7 ml of Hydrochloric acid (HCl), and then 0.05 mol solution of Erbium trioxide (Er_2O_3) was used as the dopant. The films were characterized via UV-1800 Visible Spectrophotometer, Bruker D8 Advance X-ray diffractometer with Cu Kα line (λ = 1.54056Å) in 2θ range from 10° - 90°and Scanning Electron Microscopy. The X-ray diffractometer pattern of ZrTe and Er-ZrTe thin film showed prominent crystalline peaks that are in agreement with the JCPDS card number 046-1088 and 041-1445 for ZrTe and Er-ZrTe thin film with a cubic phase indexed at (111), (200), (201), and (210) orientations and ZrTe and Er-ZrTe Films are polycrystalline with intense peaks at (111) and (210) planes at 2θ value of 26.354º and 51.360º respectively. Higher precursor temperature decreases peak intensity towards amorphous phase. The surface morphology of ZrTe thin films shows the particles are agglomerated which resulted from the formation of large grains due to effect of carbon electrode used in the process of deposition and energy band gap of 1.55 – 1.51 eV was obtained.

Keyword: *Er doped ZrTe; ECD; EDX; XRD; SEM; Optical Properties*

I. Introduction

The transition-metal dichalcogenides material have been studied extensively because of its applications in photovoltaics [1], [2], [3], [4], [5]. The transition-metal dichalcogenides materials possess different layers with the transition metal atom sandwiched between two chalcogen atoms such as S, Te or Se [6], [7], [8], [9], [10], [11] and those layers are separated by the van der Waals force, which offer new promising materials beyond graphene for exploring striking phenomena and device applications [12], [13]. Researcher have paid much attention to Zirconium-based chalcogenides material such include zirconium telluride material with great physical properties [14], [15]. Many researchers have used different technique to synthesize ZrTe thin films which includes; electrodeposition technique [16], [17] pulsed laser deposition [14], [18], [19], Sputtering [20], [21], [22]. In all these techniques mention above ECD technique is more suitable for the growth/syntheses of Erbium doped zirconium telluride thin film because it is economically friendly, easy to use, and it can be used for industrial fabrication of films within a short period of time.

This research focus on the influence of precursor temperature on erbium-doped Zirconium telluride (Er-ZrTe) using electrochemical deposition method and its application in solar cells fabrication, photovoltaic, agriculture with Zirconium (IV) oxychloride octahydrate ($ZrOCl_2$.8H2O) as the Zirconium ion source and Tellurdioxide (TeO_2), as the Telluride ion source and Erbium trioxide (Er_2O_3) as the dopant. The parameters for fabrication such as deposition potential, the

*Author to whom corresponding should be addressed (I. L Ikhioya):

*Author to whom corresponding should be addressed (C. O Obasi):

precursors temperature have been optimized at initial stages of deposition. The results reported in this research are structural, optical, EDX and scanning electron microscopy analysis

II. Materials and Method

The deposition of ZrTe and Er-ZrTe thin films the following analytically grade chemicals were used which include Zirconium (IV) oxychloride octahydrate ($ZrOCl_2.8H_2O$), Tellurdioxide (TeO_2), Hydrogen Chloride (HCl), Erbium trioxide (Er_2O_3). Others materials are; Deionized water, Power supply, Multimeter, Carbon electrode, Fluorine electrode, Fluorine doped tin oxide as substrate (FTO). The electrochemical deposition technique (ECD) was used and the bath system is composed of a source of the cation (i.e Er_2O_3, $ZrOCl_2.8H_2O$ for Er^{2+}, Zr^{2+}), a source of the anion (i.e Tellurdioxide (TeO_2 for Te^{2-}), deionized water all in 100 ml beaker, the magnetic stirrer was used to stir the reaction bath. The power supply was used to provide an electric field (DC voltage), a conducting glass was used as the cathode while the anode was carbon and fluorine electrode. Finally, uniform deposition of thin films by electrochemical deposition technique was achieved.

A. Substrate (FTO)

The substrate was a conducting glass material. The substrates were dipped in acetone, methanol, rinsed with deionized water and later ultra-sonicated for 20 min in an methanol solution. Then they were rinsed in deionized water and kept in an oven to dry.

B. The growth of Er-ZrTe thin films

The substrates were kept in vacuum to avoid contamination; using the aqueous solution of the cationic precursor of 0.1 mol solution of $ZrOCl_2.8H_2O$ while the anionic precursor was 0.15 mol solution of selenium metal powder each in 100 ml of water was added and stirred. However, Zirconium and Erbium compounds in 100 ml of water and were then stirred using the magnetic stirrer for three minutes. The FTO coated glass substrates were weighed using the electronic scale before the Erbium-doped Zirconium Selenide (Er-ZrTe) was deposited. After weighing, the conducting sides of the FTO glass substrate were determined using a multimeter. During the deposition, the target materials were poured into the beakers; about 10 ml for Erbium (Er) solution and 15 ml for Zirconium and Selenium solutions respectively. Using the forceps, the substrate was picked from the glass container and placed in-between the working electrode with its conducting side facing the Fluorine electrode and then inserted into the target material, then for 15 S, the potential drop across the thin film was measured with the help of a digital multimeter and the current passed through the sample with the help of a sensitive ammeter. The power supply was kept at a constant voltage of 10 V, after the deposition the samples were taken to the annealing machine and heated for 30 minutes to remove internal stresses. The optical absorption study of the film deposited on FTO coated glass (substrate) was carried out in the wavelength range 0f 300-1100 nm using UV-1800 spectrophotometer while the structural and were carried out using the x-ray diffractometer. The material deposited at room temperature labeled ETO and the once deposited at different precursor temperature of 50ºC, 60ºC, 70ºC, and 80ºC labeled ET1, ET2, ET3, and ET4.

C. Characterization of The Films.

The structural characterization of the films was carried out using Bruker D8 Advance X-ray diffractometer with Cu Kα line (λ = 1.54056 Å) in 2θ range from 10° - 80° the instrument helped in determining the type of lattice crystal and intensities of diffraction peaks, with the help of database software supplied by the international center of diffraction data. The quantitative analysis of the films was carried out using Energy Dispersive X-ray Analysis (EDX) for thin films to study the stoichiometry of the film. UV- visible NIR using UV-1800 visible spectrophotometer was used to obtain the absorbances of the films. Various other parameters from the absorbance were derived using the formula below (a) From the law of conservation of energy we obtained,

$$A+T+R=1 \quad (1)$$

Where A is the absorbance, R is the Reflectance, and the transmittance is T.

III. Results and Discussion

A. The Optical Analysis of ZrTe and Er-ZrTe Material

The Optical absorbance spectral of the deposited thin films were studied via Uv-visible spectrophotometer at different temperature with a wavelength range of 200 – 1100 nm. From fig. 1 there is a sharp decrease in the absorbance as the temperature increases from 50ºC - 80ºC which shown that Erbium affect the ZrTe material. ZrTe which represent the control on the plot revealed a steady decrease as the wavelength of the electromagnetic radiations increase from 450 nm to 850 nm ZrTe film absorbed more cells at the UV region of the spectrum. Er-ZrTe films absorbed more light at the UV region of

the spectrum which shown that Er-ZrTe can function in many applications such solar cells for fabrication of solar panel, photovoltaic, and supercapacitor for storage devices

The optical transmittance spectra as a function of wavelength in fig. 1b shows an inverse reaction on the

absorbance spectra in fig. 1a; the transmittance spectral transmits above 90% in UV region and near infrared region (NIR) and high transmittance at the ultraviolet region reveals how the temperature affect ZrTe because introducing Erbium to ZrTe precursor give room for free energy characteristic and increases the temperature from 50ºC – 80ºC the transmittance of the ZrTe films increases. All the samples of Erbium showed an increasing transmittance value with increasing wavelength. Er-doped samples showed significant increase in transmittance with increased temperature and the samples showed consistently increasing transmittance

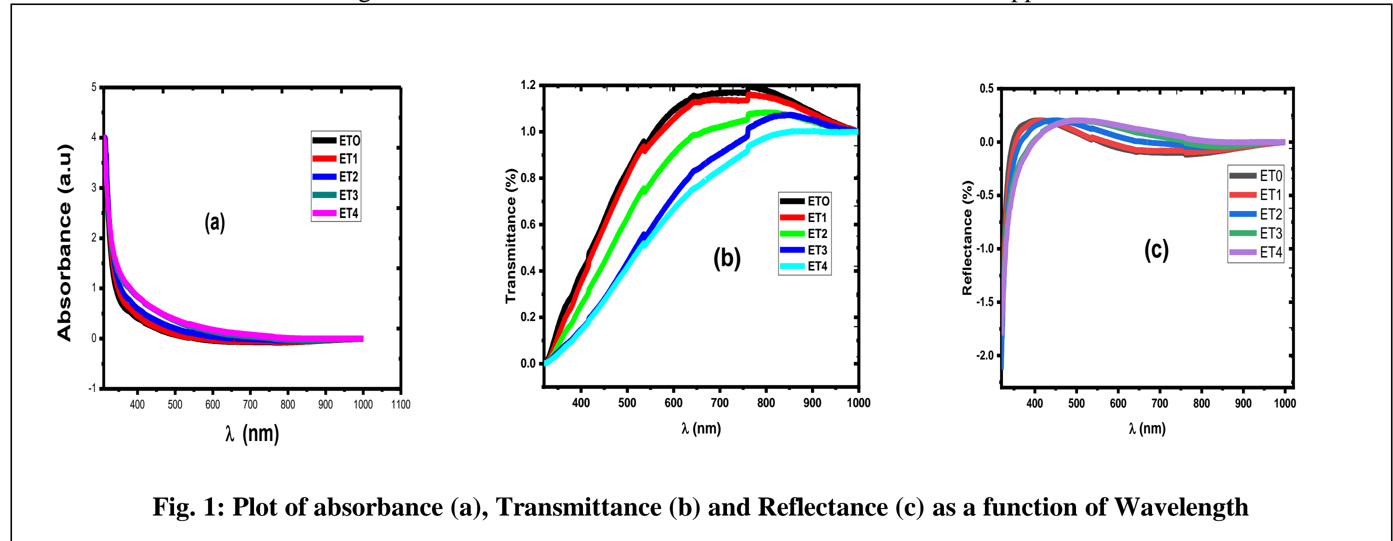

Fig. 1: Plot of absorbance (a), Transmittance (b) and Reflectance (c) as a function of Wavelength

for increasing temperature. This is attributed to the small film thickness. There was a steady increase in the transmittance spectral which revealed the ternary material like Er-ZrTe can function in mass production of solar cells materials and others application in electronic industries.

The optical reflectance spectra as a function of wavelength in fig. 1c at different temperature of 50ºC – 80ºC. From the plot ZrTe film shows an exponential decrease in the near infrared region and a steady increase in the UV region of the spectrum. All the samples showed a maximum increase of reflectance in the visible region and an exponentially decreasing reflectance in the near IR region. The exponential decrease of the film is attributed to small film thickness because of the film thickness can affect the absorption of light by the material for onward transmission and as the wavelength of electromagnetic spectrum increases the reflectance of the film increases as well.

The photon energy of the synthesized ZrTe and Er-ZrTe thin film material in fig. 2 revealed that as the absorption coefficient square increases the light radiation from the photon energy increases. The bandgap energy was determined by Tauc plot extrapolation technique, using: $(\alpha h v)^{\frac{1}{n}} = \beta(hv - E_g)$. The bandgap energy decreased in the visible and IR region and increased in the UV region. This confirms the photosensitivity of the film upon exposure to light in the IR region. The bandgap energy of 1.55 -1.51 eV was obtained

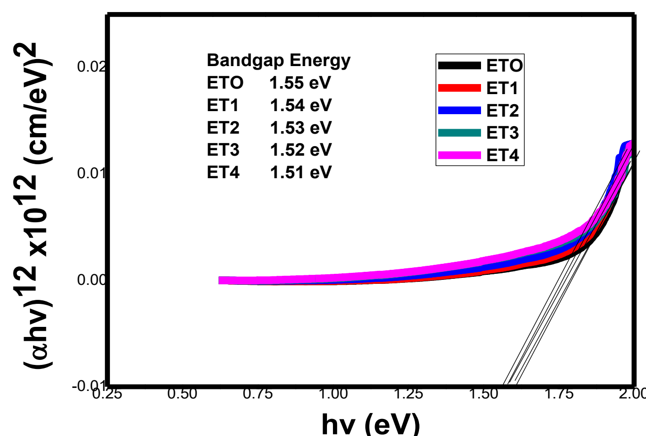

Fig. 2: Plot of absorption coefficient as a function of photon energy

The optical refractive index, extinction coefficient and optical conductivity as a function photon energy in fig.3. The plot of fig. 3a sample ETO representing ZrTe film showed a high refractive index in the UV and NIR region and a sharp decrease at the ultraviolet region and introducing Erbium as the dopant improve the refractive index of the film. In fig.3b the extinction coefficient of the thin film material synthesized at different precursor temperature increases as the light radiation fall on the surface of the film which rise to increases in the photon energy of the synthesized material and all the sample has a steady increase as the precursor temperature of the material increases (50ºC – 80ºC) and the optical conductivity of the films in fig. 3c revealed an increase in ZrTe (ETO) material and the dopant improve the optical conductivity of Er-ZrTe (ET1-ET4) thin film materials

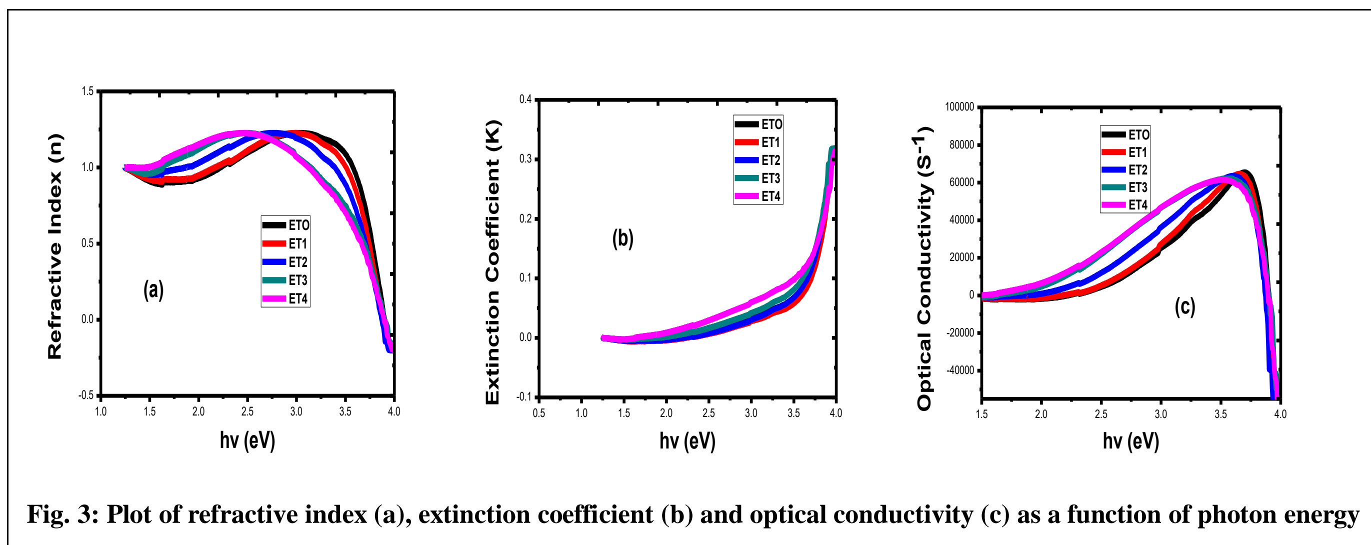

Fig. 3: Plot of refractive index (a), extinction coefficient (b) and optical conductivity (c) as a function of photon energy

The real and imaginary dielectric constant of ZrTe and Er-ZrTe thin film material as a function of photon energy in fig.4 revealed that as the temperature of Er-ZrTe films increase from 50ºC – 80ºC the electromagnetic radiation from the photon energy increases. The photon energy of the materials has a steady increase from 1.5 eV – 2.5 eV with a sharped drop in the photon energy of the film to 4.0 eV which revealed how refractive and extinction coefficient of the material can affect the real and imaginary dielectric constant of the deposited material. From the plots real and imaginary dielectric constant of

ZrTe film improve at the ultraviolet region and introducing Erbium as the dopant make a better material at 2.3 eV. In fig. 5a the real dielectric constant has a value of 0.999 and photon energy of 1.265 eV at the UV region and at the NIR region with a value of 1.503 and photon energy of 2.462 eV which results to sharp decrease of the real dielectric constant at the ultraviolet region with a value of 1.327 and photon energy of 3.404 eV. It is well noticed that increase in photon energy will result in decrease in the real dielectric constant of the synthesized material. In fig.5b the imaginary dielectric constant of the material synthesized at UV region has a value of 0.0035 and photon energy of 1.556 eV and at the NIR region has a value of 0.1655 and photon energy of 3.628 eV and at the ultraviolet region has a value of 0.0550 and photon energy of 3.866 eV and the imaginary dielectric constant increases from the UV region to the NIR region with a sharp decrease at the ultraviolet region.

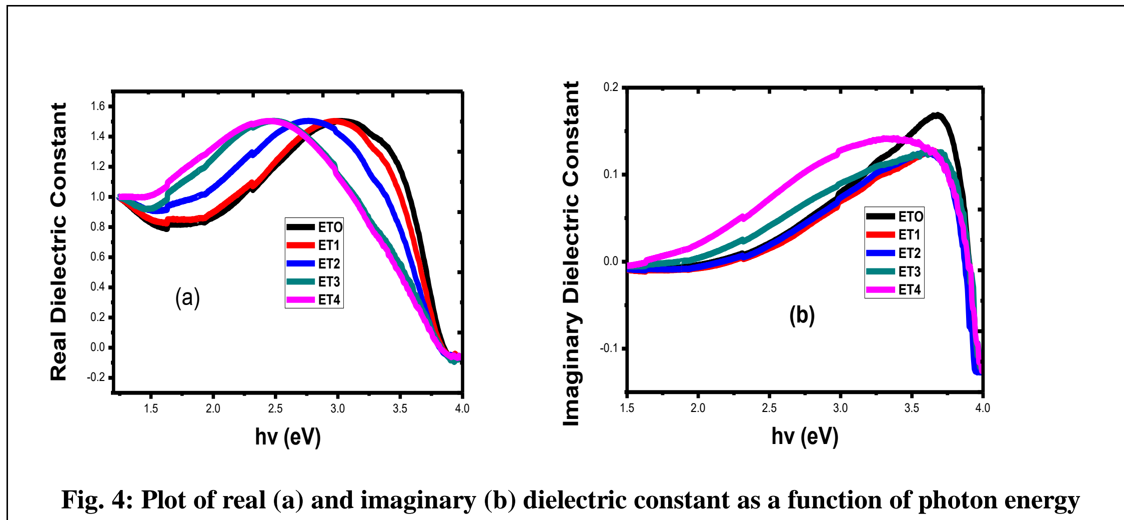

Fig. 4: Plot of real (a) and imaginary (b) dielectric constant as a function of photon energy

B. Structural Analysis of ZrTe and Er-ZrTe Material

The X-ray diffractometer pattern of ZrTe and Er-ZrTe thin film showed prominent crystalline peaks that are in agreement with the JCPDS card number 046-1088 and 041-1445 for ZrTe and Er-ZrTe thin film with a cubic phase indexed at (111), (200), (201), and (210) orientations. The XRD patterns shown in fig. 5 were obtained using the energetic $CuK_{\alpha 1}$ X-ray source (λ =1.5406 Ă) in the diffracting angle range of 15 – 80°. The ZrTe and Er-ZrTe Films are polycrystalline with intense peaks at (111) and (210) planes at 2θ value of 26.354° and 51.360° respectively. Higher precursor temperature decreases peak intensity towards amorphous phase. This is evidence of the presence of microstrain along the lattice. Average crystallite size was estimated using Scherrer's relation equ. 2

$$D = \frac{k\lambda}{\beta Cos\theta} \qquad (2)$$

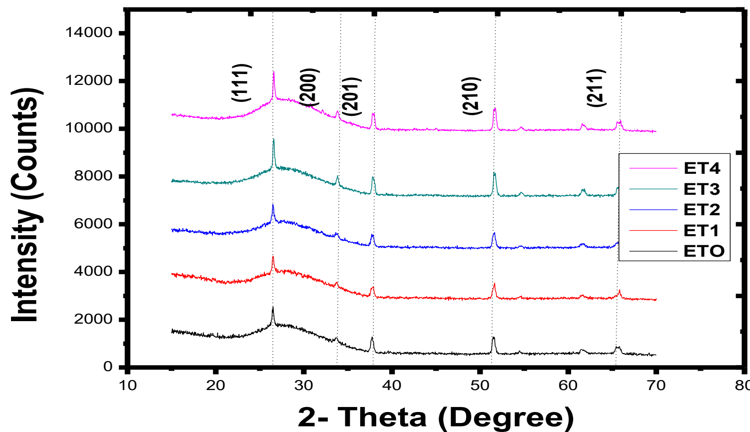

Fig. 5: XRD pattern of ZrTe and Er-ZrTe Thin Films

Sample	2θ (degree)	d (spacing) Å	Lattice constant (Å)	(β) FWHM	(hkl)	Grain Size(D) nm	Dislocation density,σ lines/m^2
ETO	26.354	1.23177	9.595764739	0.18517	111	5.38453	3.44913
ET1	33.831	19.1386	6.621168178	0.20958	200	3.80793	6.89640
ET1	37.879	1.15218	12.59781996	0.14800	201	6.96633	2.06059
ET3	57.360	0.8591	13.86580874	0.22584	210	7.07858	1.99576
ET4	65.389	0.87852	12.81689573	0.22499	211	8.55033	1.36784

C. *Surface Morphology Of ZrTe And Er-ZrTe Material*

The surface morphologies of ZrTe and Er-ZrTe thin film material in fig. 6 were obtained by Leo-Zeiss scanning electron microscopy (SEM). The surface morphology of ETO which represent ZrTe thin films shows the particles are agglomerated which resulted from the formationnn of large grains due to effect of carbon electron used in the process of deposition while doping ZrTe thin films improve the surface morphologies of the deposited samples at 50ºC and 70ºC doping with Erbium the grains size reduced at 60ºC doping its was observed in sample ET1 and ET4 a large grain size which is due to increase in temperature. All the surface morphologies are spherical in sharps and such spherical sharpes revealed the crystallites on the surface of the films. The films are free of cracks which shows that the surface of the films were smooth and visible. With a close look at Sample ET2 and ET4 though poly dispersed having a combination of ellipsoidal and spherical shape, these morphologies are suitable for solar cells, photonvoltaics and other applications in the electronic industries.

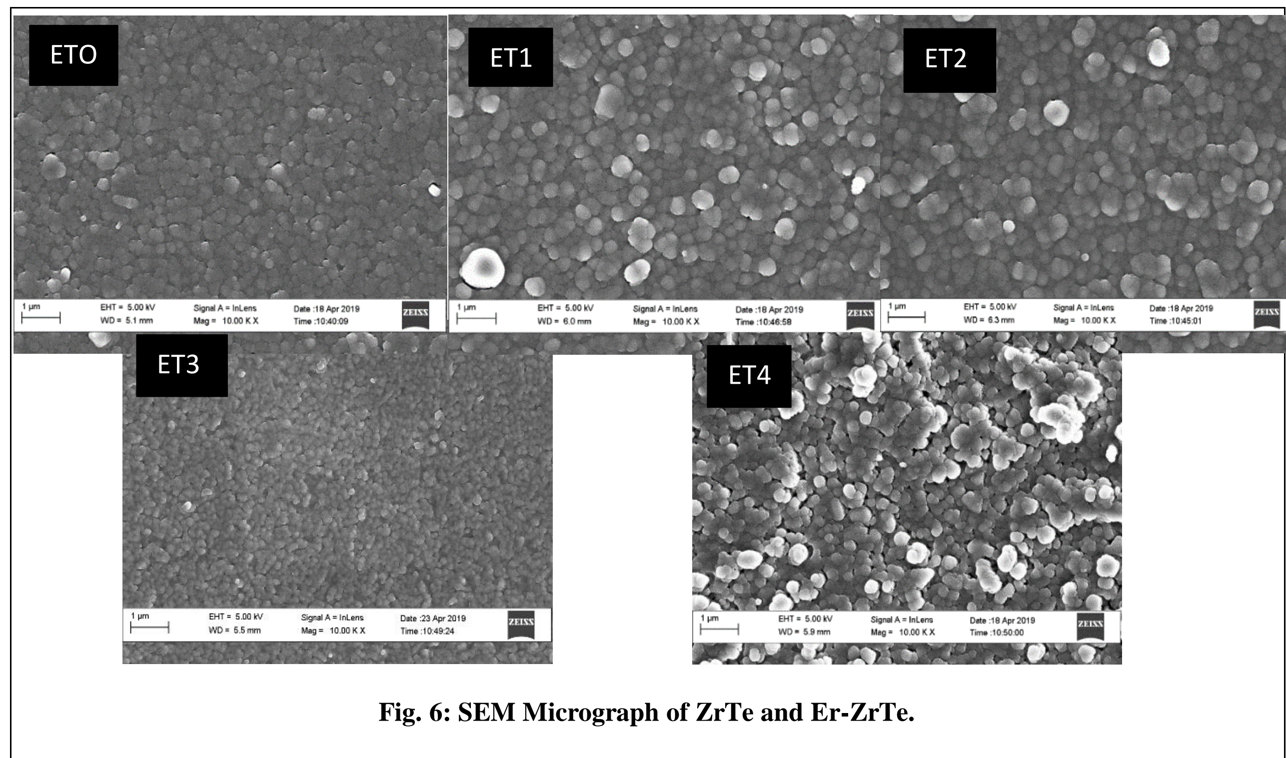

Fig. 6: SEM Micrograph of ZrTe and Er-ZrTe.

D. Elemental Study of ZrTe and Er-ZrTe Thin Films Material

The elemental analysis of ZrTe and Er-ZrTe thin films material was performed using Energy Dispersive X-ray Analysis (EDX). This unit is attached to the Scanning Electron Microscopy (SEM). JEOL-JSM 7600F Japan. It is was noticed in fig.7 the formation of ZrTe and Er-ZrTe in the EDX spectra analysis and the others element present is due to the elemental composition of the (FTO) substrate used to synthesized of thin films material

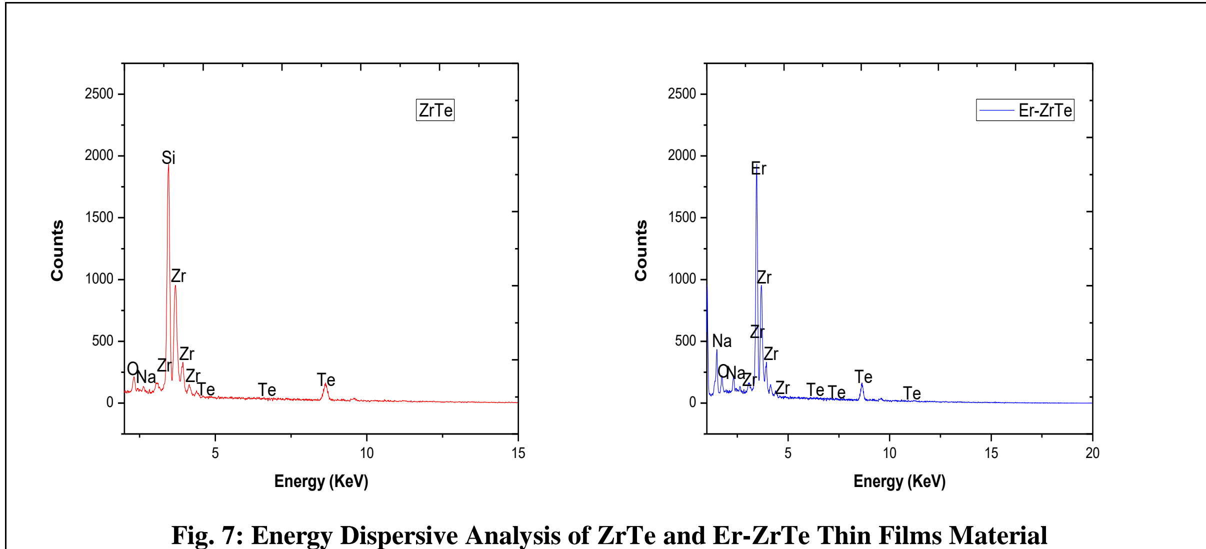

Fig. 7: Energy Dispersive Analysis of ZrTe and Er-ZrTe Thin Films Material

E. Electrical Analysis of ZrTe and Er-ZrTe Material

The Electrical study of ZrTe and Er-ZrTe thin films material in Table 2, it was noticed that the thin films material synthesized revealed increase in thickness from 142.11 – 159.15 nm with a corresponding decrease in the resistivity of the synthesized thin films material from $4.323x10^3$ – $1.292x10^3$ (Ω/cm) which resulted to corresponding increase in the conductivities of the synthesized thin films material from $0.231x10^{11}$ – $0.773x10^{11}$ $(Ωm/cm)^{-1}$.

Table 2: Electrical parameters of ZrTe and Er-ZrTe Thin Films Material

Samples	Thickness, (t) (nm)	Resistivity,(ρ) $(Ωm)^{-1}$	Conductivity, (σ) $(Ωm/cm)^{-1}$
EZO	142.11	$4.323x10^3$	$0.231x10^{11}$
EZ1	146.16	$3.340x10^3$	$0.299x10^{11}$
EZ2	149.25	$3.233x10^3$	$0.309x10^{11}$
EZ3	153.27	$2.011x10^3$	$0.497x10^{11}$
EZ4	159.15	$1.292x10^3$	$0.773x10^{11}$

IV. Conclusions

The electrochemical deposition technique has been used to growth and characterized ZrTe and Er-ZrTe thin film for photovoltaics application. The X-ray diffractometer pattern of ZrTe and Er-ZrTe thin film showed prominent crystalline peaks that are in agreement with the JCPDS card number 046-1088 and 041-1445 for ZrTe and Er-ZrTe thin film with a cubic phase indexed at (111), (200), (201), and (210) orientations. The surface morphology of ETO which represent ZrTe thin films shows the particles are agglomerated which resulted from the formationnn of large grains due to effect of carbon electrode used in the process of deposition while doping ZrTe thin films improve the surface morphologies of the deposited samples at 50°C and 70°C doping with Erbium the grains size reduced at 60°C. its was also observed in sample ET1 and ET4 a large grain size which is due to increase in temperature. There is a sharp decrease in the absorbance as the dopant concentration of Erbium increases from 1% - 4% which shown that Erbium affect the ZrTe material. ZrTe which represent the control on the plot revealed a steady decrease as the wavelength of the electromagnetic radiations increase from 250 nm to 850 nm ZrTe film absorbed more cells at the UV region of the spectrum and introducing the Erbium as the dopant change electrochemistry of the precursor. Er-ZrTe films absorbed more light at the UV region of the spectrum. The bandgap energy decreased in the visible and IR region and increased in the UV region. This confirms the photosensitivity of the film upon exposure to light in the IR region. The bandgap energy of 1.55 -1.51 eV was obtained.

Acknowledgment

We acknowledge the sponsorship of TETFUND office (UNN) through the Needs Assessment Intervention Fund. We also thank Nanosciences African Network (NANOAFNET), iThemba LABS National Research

Foundation. Also thanks to all staff of Nano Research Group University of Nigeria, Nsukka

References

[1] S. Manzeli, D. Ovchinnikov, D. Pasquier, O. V. Yazyev and A. Kis, "*2D Transition 2D Transition,*" Nat. Rev. Mater, vol. 2, p. 17033, 2017.

[2] S. Okada, T. Sambongi and M. Ido, "*Giant Resistivity Anomaly in ZrTe5.,*" J. Phys. Soc. Jpn., vol. 49, pp. 839-840, 1980.

[3] G. N. Kamm, D. J. Gillespie, A. C. Ehrlich, T. J. Wieting and F. Levy, "*Fermi Surface, Effective Masses, and Dingle Temperatures of ZrTe5 as Derived from the Shubnikov–de Haas Effect,,*" Phys. Rev. B, vol. 31, p. 7617, 1985.

[4] M. Izumi, T. Nakayama, K. Uchinokura, S. Harada, R. Yoshizaki and E. Matsuura, "*Shubnikov-de Haas Oscillations and Fermi Surfaces in Transition-Metal Pentatellurides ZrTe5 and HfTe5.*," J. Phys. C: Solid State Phys.*,* vol. 20, pp. 3691-3705, 1987.

[5] Q. Li, D. E. Kharzeev, C. Zhang, Y. Huang, I. Pletikosic, A. V. Fedorov, R. D. Zhong, J. A. Schneeloch, G. D. Gu and T. Valla, "*Chiral Magnetic Effect in ZrTe5.*," Nat. Phys., vol. 12, pp. 550-554, 2016.

[6] Y. Zhang, C. Wang, L. Yu, G. Liu, A. Liang, H. J., S. Nie, X. Sun, Y. Zang, B. Shen, J. Liu, H. Weng, L. Zhao, G. Chen, X. Jia, C. Hu, Y. Ding, W. Zhao, Q. Gao, C. Li and e. al., "*Electronic Evidence of Temperature-Induced Lifshitz Transition and Topological Nature in ZrTe5.*," Nat. Commun.*,* vol. 8, p. 15512, 2017.

[7] R. Y. Chen, Z. G. Chen, X. Y. Song, J. A. Schneeloch, G. D. Gu, F. Wang and N. L. Wang, "*Magnetoinfrared Spectroscopy of Landau Levels and Zeeman Splitting of Three-Dimensional Massless Dirac Fermions in ZrTe5.*," Phys. Rev. Lett., vol. 115, p. 176404, 2015.

[8] G. Zheng, J. Lu, X. Zhu, W. Ning, Y. Han, H. Zhang, J. Zhang, C. Xi, J. Yang, H. Du, K. Yang, Y. Zhang and M. Tian, "*Transport Evidence for the Three-Dimensional Dirac Semimetal Phase in ZrTe5.*," Phys. Rev. B, vol. 93, p. 115414, 2016.

[9] G. Manzoni, L. Gragnaniello, G. Autès, T. Kuhn, A. Sterzi, F. Cilento, M. Zacchigna, V. Enenkel, I. Vobornik, L. Barba, F. Bisti, P. Bugnon, A. Magrez, V. Strocov, H. Berger, O. Yazyev, M. Fonin, F. Parmigiani and A. Crepaldi, "*Evidence for a Strong Topological Insulator Phase in ZrTe5.,*" Phys. Rev. Lett.*,* vol. 117, p. 237601, 2016.

[10] Y. Jiang, Z. L. Dun, H. D. Zhou, Z. Lu, K. W. Chen, S. Moon, T. Besara, T. M. Siegrist, R. E. Baumbach, D. Smirnov and Z. Jiang, "*Landau-Level Spectroscopy of Massive Dirac Fermions in Single-Crystalline ZrTe5 Thin Flakes.,*" Phys. Rev. *B,* vol. 96, p. 04111, 2017.

[11] Z. Fan, Q. F. Liang, Y. B. Chen, S. H. Yao and J. Zhou, "*Transition between Strong and Weak Topological Insulator in ZrTe5 and HfTe5.*," Sci. Rep, p. 45667, 2017.

[12] Y. Sun, S. C. Wu, M. N. Ali, C. Felser and B. Yan, "*Prediction of Weyl Semimetal in Orthorhombic MoTe2*," Phys. Rev. B, vol. 92, p. 161107, 2015.

[13] Z. Wang, D. Gresch, A. A. Soluyanov, W. Xie, S. Kushwaha, X. Dai, M. Troyer, R. J. Cava and B. A. Bernevig, "*MoTe2: A Type-II Weyl Topological Metal.,*" Phys. Rev. Lett.*,* p. 056805, 2016.

[14] C. H. C. C. H. S. S. P. L. a. J.-Y. D. Huichao Wang, "*Magnetotransport Properties of Layered Topological Material ZrTe2 Thin Film,*" ACS NANO*,* pp. 1-27, 2019.

[15] Y. Liu, X. Yuan, C. Zhang, Z. Jin, A. Narayan, C. Luo, Z. Chen, L. Yang, J. Zou, X. Wu, S. Sanvito, Z. Xia, L. Li, Z. Wang and F. Xiu, "*Zeeman Splitting and Dynamical Mass Generation in Dirac Semimetal ZrTe5.,*" Nat. Commun., vol. 7, p. 12516, 2016.

[16] I. L. IKHIOYA, "*OPTICAL AND ELECTRICAL PROPERTIES OF ZnTe THIN FILMS USING ELECTRODEPOSITION TECHNIQUE*," International Journal of Innovation and Applied Studies, vol. 12, no. 2, pp. 369-373, 2015.

[17] I. L. e. a. Ikhioya, "*Effect Of Temperature On SnZnSe Semiconductor Thin Films For Photovoltaic Application*," SSRG International Journal of Applied Physics (SSRG-IJAP), vol. 6, no. 2, pp. 55-67, 2019.

[18] W. L. Zhu, J. B. He, S. Zhang, D. Chen, L. Shan, Z. A. Ren and G. F. Chen, "*Magnetotransport Properties of the New-Type Topological Semimetal ZrTe.,*" arXiv:1707.00942.*,* pp. 432-442, 2016.

[19] P. Tsipas, D. Tsoutsou, S. Fragkos, R. Sant, C. Alvarez, H. Okuno, G. Renaud, R. Alcotte, T. Baron and A. Dimoulas, "*Massless Dirac Fermions in ZrTe2 Semimetal Grown on InAs (111) by Van Der Waals Epitaxy.*," ACS Nano, vol. 12, pp. 1689-1703, 2018.

[20] Y. M. A. D. P. S. CAUNE, "*DEPOSITION AND CHARACTERIZATION OF ZrTex THIN FILMS,*" Thm Solid Films, vol. 174, pp. 289-293, 1989.

[21] X. B. Li, W. K. Huang, Y. Y. Lv, K. W. Zhang, C. L. Yang, B. B. Zhang, Y. B. Chen, S. H. Yao, J. Zhou, M. H. Lu, L. Sheng, L. S. C., J. F. Jia, Q. K. Xue, Y. F. Chen and D. Y. Xing, "*Experimental Observation of Topological Edge States at the Surface Step Edge of the Topological Insulator ZrTe5.,*" Phys. Rev. Let*,* p. 176803, 2016.

[22] R. Wu, J. Z. Ma, S. M. Nie, L. X. Zhao, X. Huang, J. X. Yin, B. B. Fu, P. Richard, G. F. Chen, Z. Fang, X. Dai, H. M. Weng, T. Qian, H. Ding and S. H. Pan, "*Evidence for Topological Edge States in a Large Energy Gap near the Step Edges on the Surface of ZrTe5.,*" Phys. Rev. X, vol. 6, p. 021017, 2016.

[23] M. F. P. a. G. C. Birkholz, "*Thin film analysis by X-ray scattering,*" Weinhein: Wiley-VCH Boston: Academic Press. , pp. 466-478, 2015.